analytical chemistry

Article

pubs.acs.org/ac

Toward the Accurate Analysis of C_1−C_4 Polycyclic Aromatic Sulfur Heterocycles

Christian Zeigler, Nicholas Wilton, and Albert Robbat, Jr.*

Department of Chemistry, Tufts University, 62 Talbot Avenue, Medford, Massachusetts 02155, United States

ABSTRACT: Polycyclic aromatic sulfur heterocycles (PASH) are sulfur analogues of polycyclic aromatic hydrocarbons (PAH). Alkylated PAH attract much attention as carcinogens, mutagens, and as diagnostics for environmental forensics. PASH, in contrast, are mostly ignored in the same studies due to the conspicuous absence of gas chromatography/mass spectrometry (GC/MS) retention times and fragmentation patterns. To obtain these data, eight coal tar and crude oils were analyzed by automated sequential GC−GC. Sample components separated based on their interactions with two different stationary phases. Newly developed algorithms deconvolved combinatorially selected ions to identify and quantify PASH in these samples. Simultaneous detection by MS and pulsed flame photometric detectors (PFPD) provided additional selectivity to differentiate PASH from PAH when coelution occurred. A comprehensive library of spectra and retention indices is reported for the C_1−C_4 two-, three-, and four-ring PASH. Results demonstrate the importance of using multiple fragmentation patterns per homologue (MFPPH) compared to selected ion monitoring (SIM) or extraction (SIE) to identify isomers. Since SIM/SIE analyses dramatically overestimate homologue concentrations, MFPPH should be used to correctly quantify PASH for bioavailability, weathering, and liability studies.

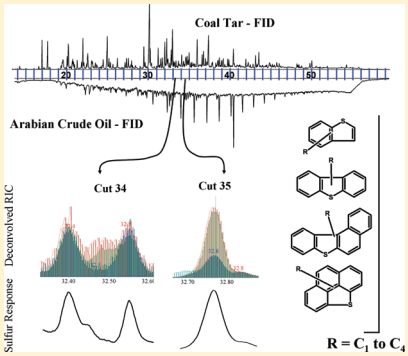

Polycyclic aromatic hydrocarbons (PAH) are threats to human health and the environment.[1−9] PAH and their alkylated analogues serve as forensic markers during site investigation, cleanup, and monitoring.[10−24] The U.S. Environmental Protection Agency (EPA) estimates the toxic hazard of contaminated soils, sediment, and marine life by quantifying the so-called $\sum PAH_{34}$, viz., 18 parent PAH and 16 C_1−C_4 alkylated homologues.[25−27] If the toxic unit exceeds the site-specific action level, remedial action is required.[28,29]

Gas chromatography/mass spectrometry (GC/MS) is the only analytical technique that can provide unambiguous identification of PAH but only if mass spectra are known and matrix organics do not interfere with compound assignments. Accurate GC/MS data are critical to site assessments, remedial outcomes, and liability apportionments. Due to the complexity of coal tar and petroleum, most analysts use selected ion monitoring (SIM) or extraction (SIE) to collect the molecular ion signal and, perhaps, one confirming ion to identify alkyl PAH. Others collect full scan data but use only the fragmentation pattern of one isomer to assign compounds to a specific homologue. We recently described the errors associated with both approaches, namely, overestimation of target compound concentrations by SIM and underestimation of the concentration when a single fragmentation pattern is used to quantify homologues.[30] Both approaches ignore differences in the spectra of isomers and common ion effects from matrix compounds that lead to inaccurate compound assignments. For example, C_4 naphthalene and three-ring polycyclic aromatic sulfur heterocycles (PASH) coelute and have the same molecular ion.

To address these shortcomings, we used GC−GC/MS to build a retention time and mass spectrometry library for C_1−C_4 naphthalenes, fluorenes, phenanthrenes, pyrenes, and chrysenes found in coal tar and crude oil. Automation of this technique sequentially transferred one minute sample portions from the first to the second column after the previous sample eluted from column 2. "Heart-cuts" often contained dozens of compounds, which separated from one another due to selectivity differences between the two stationary phases. When this occurred, GC−GC/MS produced clean spectra; however, many PAH coeluted with sulfur aromatics.

Recently, we studied the retention behavior of 119 three-ring to six-ring PASH on four different stationary phases to determine the optimum combination of columns to analyze PASH by GC−GC/MS.[31] Although the work produced the most comprehensive PASH retention index data to date, our results were limited to mostly parent compounds. Since almost no retention time and mass spectrometry data exists for the C_2−C_4 homologues, scientists and regulators pay little attention to these compounds despite the fact they bioaccumulate,[32−34] are toxic,[35] mutagenic,[36,37] carcinogenic,[38−40] and often are used as forensic biomarkers to evaluate weathering.[41] Furthermore, the EPA does not include alkylated PASH in their narcosis model, which may lead to toxicity calculations that underestimate the true risk of a site.

This study's main objective is to determine the retention window in which each alkylated PASH homologue elutes and

Received: October 27, 2011
Accepted: January 17, 2012

   dx.doi.org/10.1021/ac202845x | *Anal. Chem.* XXXX, XXX, XXX−XXX

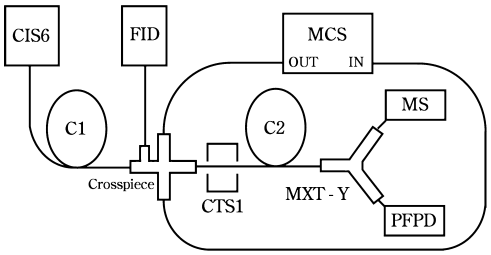

Figure 1. Diagram of GC−GC/MS−PFPD instrumentation.

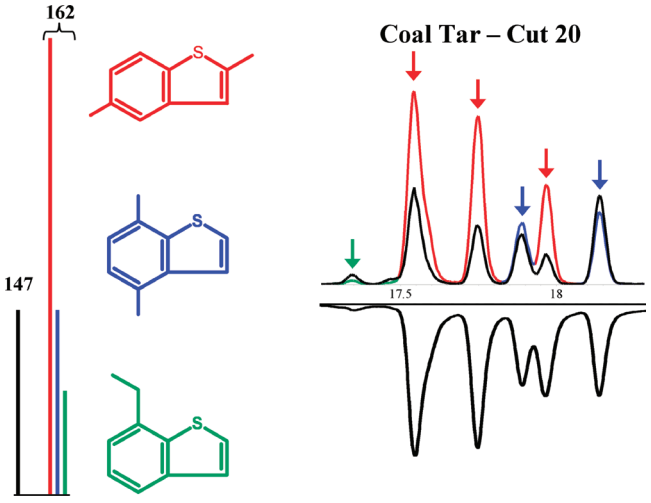

Figure 2. Stick diagram for expected ion ratios of 2,5-dimethyl- (red), 4,7-dimethyl- (blue), and 7-ethylbenzothiophene (green) at m/z 147 (black) and m/z 162. Also shown are the corresponding reconstructed ion current chromatograms for cut 20 (top); see arrows for peak assignments. The bottom chromatogram is the simultaneous pulse flame photometric sulfur-specific response.

to obtain the mass spectra needed to identify them. Another objective is to document the inaccuracies associated with SIM/SIE analyses and to prove the level of misestimation is unacceptable. To increase mass on-column and to remove spectral interferences from nonaromatics such as aliphatic and polar compounds, coal tar and crude oil were fractionated using silica column chromatography prior to analysis by GC−GC/MS. Simultaneous pulsed flame photometric detection (PFPD) provided the selectivity needed to differentiate PASH from PAH. Rationalization of mass spectral fragmentation patterns permitted the combinatorial selection of ions used to detect alkylated two-, three-, and four-ring isomers in real-world samples as opposed to standards. Results demonstrate the importance of using multiple fragmentation patterns per homologue (MFPPH) to quantify PASH.

EXPERIMENTAL SECTION

Materials and Reagents. Merey and Orinoco crude oils were obtained from ONTA (Toronto, Ontario, Canada). Zhendi Wang, Environment Canada (Ottawa, Ontario, Canada), provided a 23.2% by weight weathered Arabian crude oil. Two former manufactured gas plants in North Carolina and New York provided fresh and weathered coal tar samples. Alberta Innovates (Edmonton, Alberta, Canada) provided a 12% by weight Athabasca oil sands.

Silica gel (grade 644, 100−200 mesh, 150 Å pore size) and sodium sulfate (>99.4%) were purchased from Sigma-Aldrich (St. Louis, MO). Sigma-Aldrich and Fisher Scientific (Pittsburgh, PA) supplied the solvents, purity >99.5%.

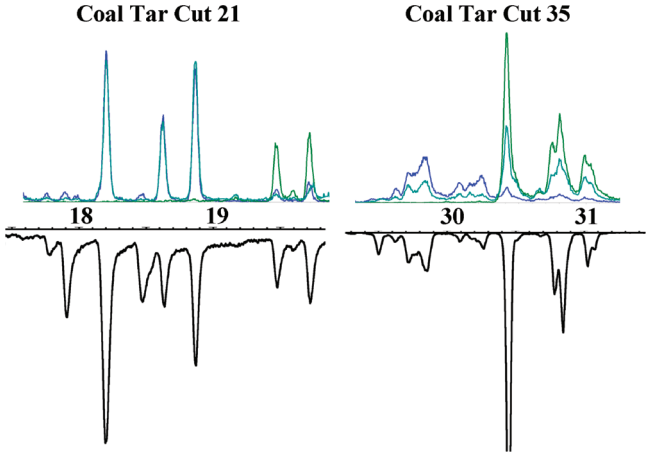

Figure 3. C_2 (blue) and C_3 (green) molecular ion traces (top) for two-ring (cut 21) and three-ring (cut 35) PASH. Confirmation ions for C_2 two-ring (m/z 147) and C_2 three-ring (m/z 211) are shown in turquoise for cuts 21 and 35, respectively. These ions are also minor ions of the C_3 homologue. PFPD response (bottom) confirms the presence of sulfur compounds.

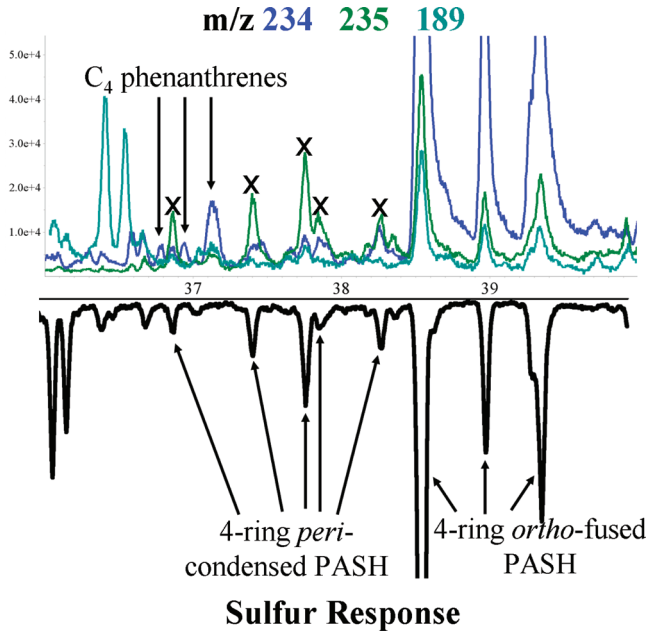

Figure 4. Extracted ion current profiles (top) for C_4 phenanthrene and four-ring ortho-fused PASH base ion (blue) and confirming ions (green and turquoise) in coal tar. Arrows and ×'s indicate C_4 phenanthrene and C_2 four-ring peri-condensed PASH, respectively. PFPD response (bottom) indicates sulfur compounds.

Purchased from Airgas (Billerica, MA) were liquid nitrogen and ultrahigh purity helium, hydrogen, and compressed air.

Fractionation. Prior to fractionation, three equivalent volumes of methylene chloride were used to wash 100 mL of silica gel, which was activated overnight at 180 °C. Approximately 3 g of silica gel was dry packed into a 20 cm ×1 cm glass column obtained from EST Chemicals (Tucson, AZ), which produced a 13 cm column topped with ∼1 cm of sodium sulfate. A volume of 20 mL of hexane conditioned the column prior to loading 40 mg of sample. Then 20 mL of hexane removed aliphatic compounds followed by 20 mL of 50% hexane/50% methylene chloride and 30 mL of toluene to elute aromatics. A nitrogen line connected to the column supplied

dx.doi.org/10.1021/ac202845x | Anal. Chem. XXXX, XXX, XXX−XXX

Table 1. Fragmentation Patterns of PASH Detected in Coal Tar[1] and Crude Oil[2] Samples Based on Ions Selected through the Combinatorial Library Building Process

isomers represented	fragmentation pattern[a]	base ion (% RA)	confirmation ions (% RA)			
C_1 Two-Ring PASH						
2-, 3-, 4-, 5-, and 6-methyl	C_1 BT A[1,2]	147 (100)	148 (84)	149 (13)	45 (13)	74 (10)
C_2 Two-Ring PASH						
2,7-, 2,5-, and 3,6-dimethyl	C_2 BT A[1,2]	162 (100)	161 (87)	147 (34)	163 (14)	80 (13)
4,7- and 6,7-dimethyl	C_2 BT B[1,2]	162 (100)	147 (100)	84 (82)	161 (70)	163 (13)
7-ethyl	C_2 BT C	147 (100)	162 (44)	148 (11)		
unknown isomers	C_2 BT D[1,2]	161 (100)	162 (48)	80 (34)	147 (21)	
C_3 Two-Ring PASH						
2,5,7-trimethyl	C_3 BT A[1,2]	176 (100)	161 (75)	175 (70)	177 (14)	
7-ethyl-2-methyl, 2-ethyl-7-methyl, 2-ethyl-5-methyl	C_3 BT B [1,2]	161 (100)	176 (50)	162 (12)		
2-propyl	C_3 BT C	147 (100)	176 (28)	148 (14)		
unknown isomers	C_3 BT D[1,2]	161 (100)	176 (92)	175 (41)	177 (14)	162 (12)
unknown isomers	C_3 BT E[1]	161 (100)	162 (48)	80 (34)	147 (21)	
C_4 Two-Ring PASH						
2,3- and 2,7-diethyl, 2-ethyl-5,7-dimethyl	C_4 BT A[1,2]	175 (100)	190 (57)	176 (15)	160 (10)	
unknown isomers	C_4 BT B[2]	175 (100)	176 (42)	190 (39)	161 (35)	
unknown isomers	C_4 BT C[1,2]	190 (100)	175 (99)	189 (40)	191 (15)	176 (14)
unknown isomers	C_4 BT D[1,2]	161 (100)	190 (35)	175 (23)	162 (19)	
C_1 Three-Ring PASH						
unknown isomer	C_1 D A[1]	198 (100)	197 (70)	199 (19)		
3-methyl and 4-methyl	C_1 D B[1]	198 (100)	197 (50)	199 (17)	99 (10)	
C_2 Three-Ring PASH						
dimethyl isomers except 1,2; 1,3; 2,3	C_2 D A[1,2]	212 (100)	211 (45)	197 (20)	213 (17)	
1,2; 1,3; 2,3-dimethyl	C_2 D B[1,2]	212 (100)	197 (55)	211 (37)	213 (25)	
ethyl isomers	C_2 D C[2]	197 (100)	212 (52)	184 (31)		
unknown isomers	C_2 D D[1,2]	197 (100)	212 (70)	213 (12)		
C_3 Three-Ring PASH						
4-ethyl-6-methyl	C_3 D A[1,2]	211 (100)	226 (78)	212 (17)	227 (13)	
1,4,8; 1,4,6; 1,2,4; 2,4,6; 2,6,7; and 3,4,6;-trimethyl	C_3 D B[1,2]	226 (100)	211 (45)	227 (20)	212 (10)	
unknown isomers	C_3 D C[1]	226 (100)	211 (34)	227 (18)		
unknown isomers	C_3 D D[2]	226 (100)	211 (90)	227 (20)	212 (20)	
C_4 Three-Ring PASH						
1,4,6,8; 2,4,6,8; 2,4,6,7; 1,3,6,8-tetramethyl	C_4 D A[2]	240 (100)	225 (63)	241 (20)	239 (18)	226 (10)
unknown isomer	C_4 D B[2]	240 (100)	225 (44)	241 (19)	119 (13)	120 (12)
2,4-dimethyl-6-ethyl	C_4 D C[2]	225 (100)	240 (69)	226 (16)	209 (12)	241 (11)
4,6-diethyl	C_4 D D[2]	225 (100)	240 (89)	226 (27)	210 (22)	241 (15)
unknown isomers	C_4 D E[2]	240 (100)	225 (81)	226 (20)	241 (16)	210 (9)
C_1 Four-Ring ortho-Fused PASH						
unknown isomers	C_1 4-PASH A[2]	248 (100)	247 (30)	249 (20)	124 (10)	
C_2 Four-Ring ortho-Fused PASH						
unknown isomers	C_2 4-PASH B[2]	262 (100)	261 (24)	263 (21)	247 (15)	
C_3 Four-Ring ortho-Fused PASH						
unknown isomers	C_3 4-PASH A[2]	276 (100)	261 (32)	277 (22)	275 (14)	138 (10)
C_4 Four-Ring ortho-Fused PASH						
unknown isomers	rationalized ions	290	275	291	289	145
C_1 Four-Ring peri-Condensed PASH						
unknown isomers	C_1 4-*peri*-PASH A[1]	222 (100)	221 (80)	223 (20)	111 (25)	
C_2 Four-Ring peri-Condensed PASH						
unknown isomers	C_2 4-*peri*-PASH A[1]	236 (100)	235 (53)	237 (22)	234 (17)	117 (13)
C_3 Four-Ring peri-Condensed PASH						
unknown isomers	C_3 4-*peri*-PASH A[1]	250 (100)	249 (40)	235 (28)	251 (20)	248 (10)
unknown isomers	C_3 4-*peri*-PASH B[1]	250 (100)	235 (67)	251 (22)	249 (20)	248 (13)
C_4 Four-Ring peri-Condensed PASH						
unknown isomers	rationalized ions	264	249	263	256	132

[a]BT = benzothiophene. D = dibenzothiophene.

sufficient head pressure to maintain a constant flow of ~1 drop/s. The methylene chloride and toluene fractions were concentrated to ~2 mL by passing nitrogen over the sample.

Instrumentation. Figure 1 shows schematically the GC–GC/MS–PFPD. The first column (C1, 30 m × 0.25 mm i.d. × 0.25 μm Rxi-17Sil-MS from Restek) was connected to a CIS-6

dx.doi.org/10.1021/ac202845x | Anal. Chem. XXXX, XXX, XXX–XXX

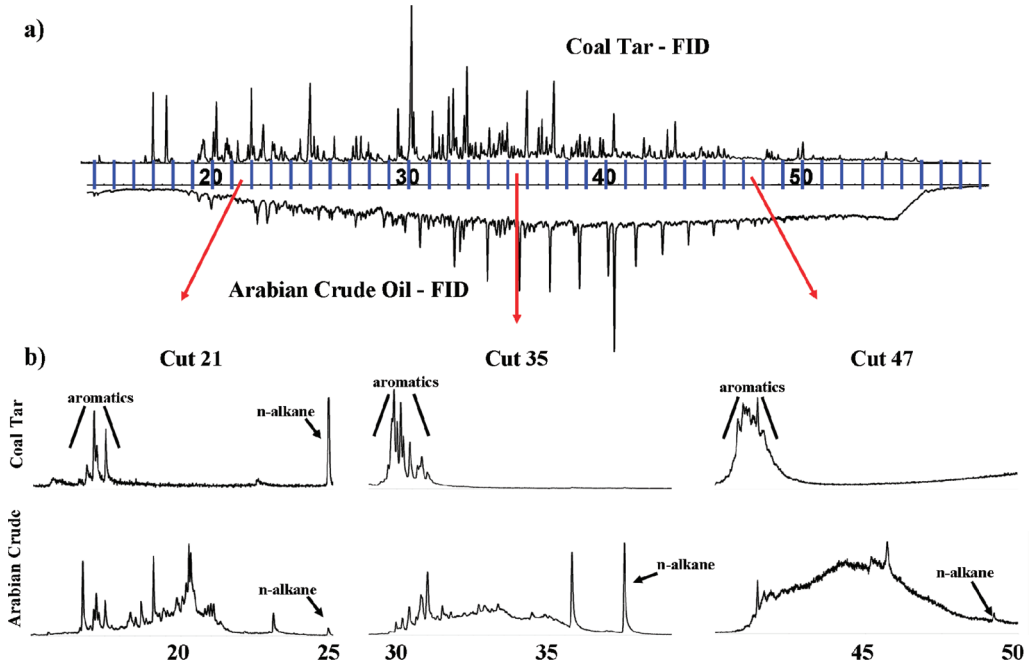

Figure 5. (a) GC/FID chromatogram of coal tar (top) and crude oil (bottom). Vertical lines represent heart-cut time periods of 1 min. (b) Coal tar (top) and Arabian crude oil (bottom) heart-cuts 21, 35, and 47.

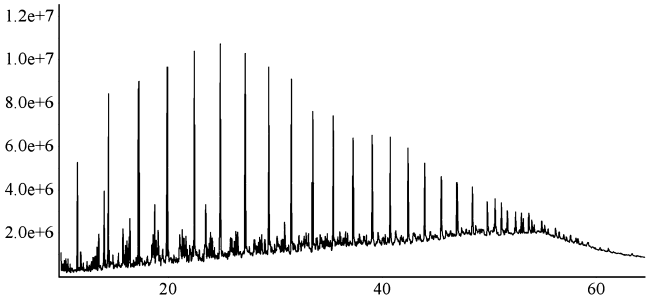

Figure 6. Total ion chromatogram of the same oil shown in Figure 5 (bottom) without fractionation.

Table 2. PASH Retention Windows Using the Andersson (PASH) (Ref 42) and Lee (PAH) (Ref 43) Index Systems

	Andersson index		Lee index	
homologue	from	to	from	to
	Two-Ring PASH			
C_1	216.9	225.2	217.5	225.3
C_2	235.4	252.8	234.9	251.3
C_3	252.8	271.8	251.3	269.1
C_4	271.1	289.8	268.5	286.1
	Three-Ring PASH			
C_1	315.1	336.0	309.6	329.4
C_2	331.2	355.4	324.8	347.9
C_3	347.3	371.5	340.0	363.4
C_4	363.4	389.9	355.2	381.2
	Four-Ring PASH			
C_1	412.4	431.8	402.3	421.6
C_2	429.6	446.8	419.5	436.6
C_3	442.5	472.5	431.2	462.0
	Four-Ring peri-Condensed PASH			
C_1	367.4	387.5	359.5	378.9
C_2	384.5	399.6	375.9	390.5
C_3	403.9	415.9	394.4	405.8

Table 3. Percent Differences Produced by SIE versus MFPPH Analysis of the Same Data File[a]

	% overestimation			
	coal tar		crude oil	
homologue	no window	with window	no window	with window
C_1 two-ring PASH	14	0	false positive	false positive
C_2 two-ring PASH	91	20	false positive	0
C_3 two-ring PASH	561	4	166	13
C_4 two-ring PASH	1615	20	92	13
C_1 three-ring PASH	11	4	70	19
C_2 three-ring PASH	8	3	42	18
C_3 three-ring PASH	145	6	23	18
C_4 three-ring PASH	547	38	false positive	false positive
C_1 four-ring *peri*-PASH	55	19	false positive	false positive
C_2 four-ring *peri*-PASH	48	21	false positive	false positive
C_3 four-ring *peri*-PASH	653	122	461	219
C_4 four-ring *peri*-PASH	false positive	false positive	false positive	false positive
C_1 four-ring PASH	16	9	115	33
C_2 four-ring PASH	31	20	33	3
C_3 four-ring PASH	344	37	56	43
C_4 four-ring PASH	false positive	false positive	false positive	false positive

[a]See Table 2 for retention windows.

injector and a five-port crosspiece (Gerstel, Mulheim an der Ruhr, Germany). Ten percent of the flow from C1 was diverted by the crosspiece through a 40 cm × 0.05 mm i.d. fused-silica capillary to a flame ionization detector (FID) operated at 250 °C. The FID used 40 mL/min H_2, 450 mL/min air, and 40 mL/min He. The Gerstel MCS mass flow controller supplied countercurrent

dx.doi.org/10.1021/ac202845x | *Anal. Chem.* XXXX, XXX, XXX–XXX

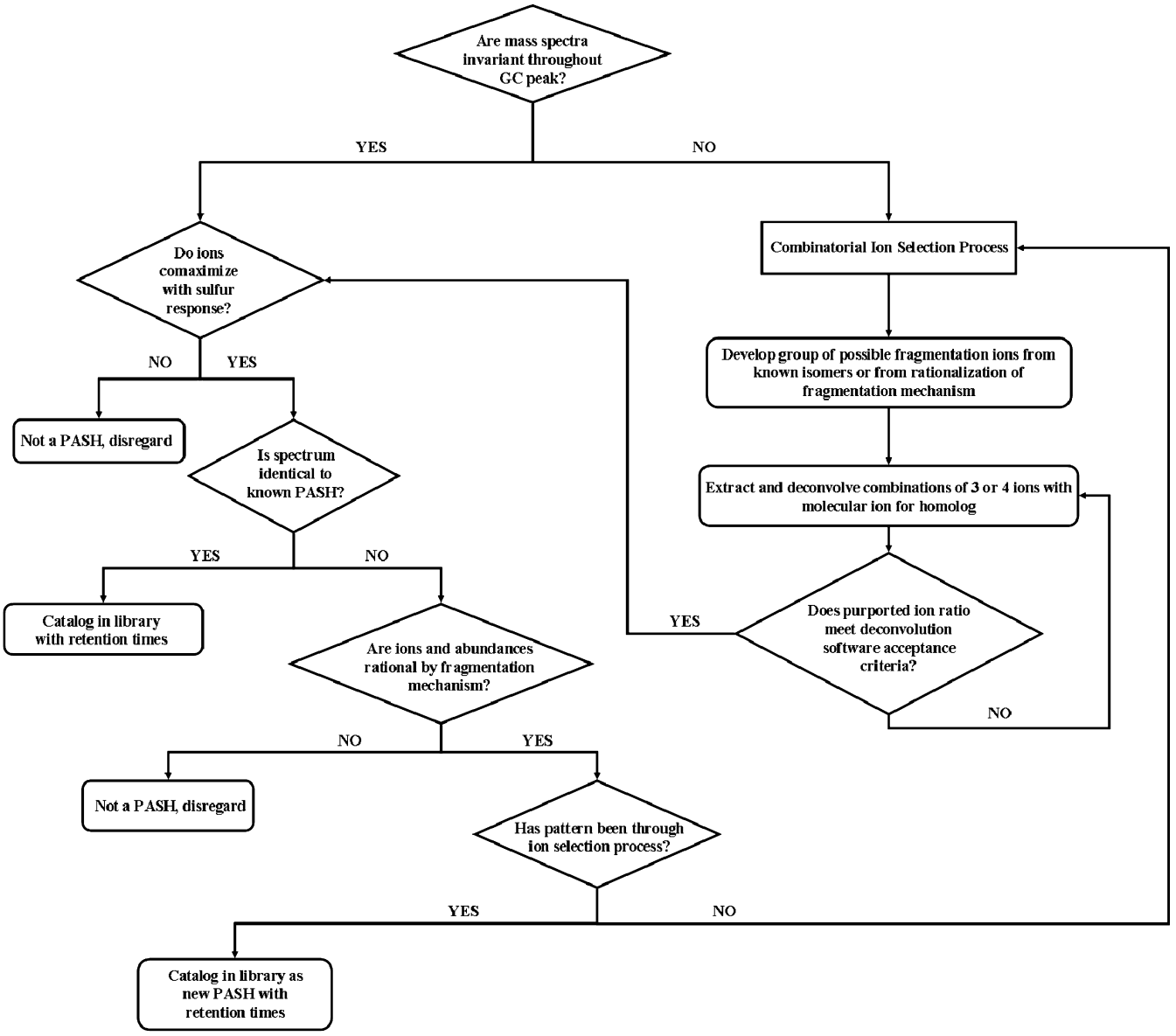

Figure 7. Flowchart of the library building process.

flow to the crosspiece. Its purpose was to divert flow to waste (flow on) or to the second column (flow off). The second column (C2, a Restek 30 m × 0.25 mm i.d. × 0.25 μm Rtx-5MS stationary phase), housed in a second oven, was connected to the crosspiece through the Gerstel CTS1 cryotrap. The opposite end of C2 joined to a Restek MXT "Y-union". Two 0.5 m × 0.10 mm i.d. and 0.18 mm i.d. deactivated fused-silica columns connected the union to the MS (model 5973, Agilent Technologies, Santa Clara, CA) and PFPD (OI Analytical Inc., Houston, TX), respectively. Agilent's Chemstation software acquired data from all three detectors. Full scan data was obtained between 50 and 400 amu at 5 scans/s. The 70 eV ion source and quadrupole temperatures were 230 and 150 °C, respectively. The PFPD pulsed at 3.8 Hz and used 14 mL/min H_2, 12 mL/min air, and 15 mL/min He.

To fully profile oil and coal tar samples, the Gerstel MPS2 autosampler was programmed to make 2 μL splitless injections. The injection port was ramped from −20 to 330 °C (5 min) at 12 °C/s. Heart-cuts started at 11 min and ended at 61 min per C1 runtime. Each heart-cut transferred a 1 min sample portion. Subsequent injections occurred at the end of the C2 runtime. The GC software determined the initial head pressure (268 kPa, 1 min) based on the C1 plus C2 dimensions (60 m), initial temperature (60 °C), column flow (2.43 mL/min, which was the optimized GC/MS−PFPD carrier gas flow), and ambient outlet pressure (101 kPa). The pressure at the crosspiece was 165 kPa after turning off the countercurrent flow and pressure and allowing the system to equilibrate. Maintaining this pressure at the crosspiece during C1 sample separation provided constant flow independent of heart-cut activity. To ensure the crosspiece pressure was 165 kPa and independent of programming temperatures, the C1 temperature was set to 330 °C, with the inlet pressure changed manually until the crosspiece was 165 kPa. At this point, the inlet pressure was 389 kPa. The pressure programming rate was determined by mirroring the temperature programming rate so that both started and ended at the same time, viz., [(389−268 kPa)/(330−60 °C)] × 5 °C/min, or 2.5 kPa/min.

Until the heart-cut started, the MCS maintained constant crosspiece pressure (165 kPa) and carrier gas flow (10 mL/min). Three minutes prior to the heart-cut, the cryotrap programmed

dx.doi.org/10.1021/ac202845x | Anal. Chem. XXXX, XXX, XXX−XXX

from 300 to −100 °C (5 min). To make the heart-cut, countercurrent flow was set to off. After sample transfer, initial countercurrent flows and pressures were reestablished. One minute later the sample was thermally desorbed (300 at 12 °C/s) onto C2. Upon desorption, the crosspiece pressure ramped from 165 to 305 kPa at 2.9 kPa/min to provide constant carrier gas flow through C2 at 2.43 mL/min. At the same time, the C1 inlet pressure decreased from the pressure at the point of heart-cut to 20 at 100 kPa/min, which caused the carrier gas to reverse direction and backflush through the injector port. The temperature program for both columns started at 60 °C (1 min), ramped to 330 at 5 °C/min, upon sample injection onto C1 or thermal desorption onto C2. The separation time for each column was 64 min. The total GC−GC cycle time was the time to the C1 heart-cut plus the 1 min transfer, 1 min system equilibration, and C2 separation times.

For one-dimensional GC/MS−PFPD analysis, the Rtx-5 column connected directly to the CIS4 inlet on the second GC, which provided constant flow of 2.43 mL/min He. Otherwise, the instrument conditions were the same as described above.

Retention Index. PASH retention windows using the Andersson (PASH)[42] and Lee (PAH)[43] index systems are calculated as follows:

$$\text{index} = \text{index}_{\text{IS}} + \left\{ \left[\frac{t_r(\text{compound}) - t_r(\text{IS})}{t_r(\text{IS}+1) - t_r(\text{IS})} \right] \times 100 \right\}$$

The index_{IS} values are 200, 300, 400, and 500 for naphthalene, phenanthrene, chrysene, and benzo[*ghi*]perylene in the Lee system, and 200, 300, 400, and 450 for benzo[*b*]thiophene, dibenzothiophene, benzo[*b*]naphtho[2,1-*d*]thiophene, and benzo[2,3]phenanthro[4,5-*bcd*]thiophene in the Andersson system. t_r(compound) is the retention time for the compound of interest, t_r(IS) and t_r(IS + 1) are the retention times of the brackets eluting before and after the compound of interest.

Software. New spectral deconvolution algorithms[44] were used in this investigation. The NIST05 and Wiley mass spectrometry libraries confirmed compound identities where possible.

RESULTS AND DISCUSSION

The stick diagram in Figure 2 illustrates the *m*/*z* 147 (black) to 162 relative abundance (RA) for 2,5-dimethylbenzothiphene (red), 4,7-dimethylbenzothiophene (blue), and 7-ethylbenzothiophene (green). Also shown are the selected ion traces for these ions in heart-cut 20 from coal tar. Of the 21 possible ethyl and dimethyl benzothiophenes, we found three isomers whose ion ratios are 40%, see red peaks. Two additional isomers have a RA of 100%, see blue peaks. We found only one of the six possible ethylated isomers at 200% RA, see green peak. Analysis of all heart-cut data revealed 14 C_2 benzothiophenes in the sample. Since analysts select at most two ions to establish compound presence, choosing one ratio over the other two results in loss of analyte and underestimation of the homologue concentration. In fact, a fourth pattern identified other C_2 isomers in which neither ion is the base ion, see Table 1.

Some analysts ignore ion ratios completely and rely solely on two ions comaximizing to determine compound presence. Figure 3 displays the C_2 (blue) and C_3 (green) molecular ion traces for two-ring (cut 21) and three-ring (cut 35) PASH found in the same sample. Below the ion traces are the PFPD responses confirming the presence of sulfur compounds. Identification of the C_n homologue by SIM or SIE will include ion signals from the C_{n+1} PASH. For example, *m*/*z* 162 (blue) and *m*/*z* 147 (turquoise) are major and minor ions for the two-ring C_2 and C_3 PASH, respectively, see cut 21. Similarly, *m*/*z* 212 (blue) and *m*/*z* 211 (turquoise) are the dominant and minor ions for three-ring C_2 and C_3 PASH, respectively, see cut 35. Ignoring ion ratios will produce higher C_n homologue concentrations for each parent PASH than are in the sample.

Figure 4 (top) shows the molecular ion at *m*/*z* 234 (blue) and confirming ions at *m*/*z* 235 (green) and 189 (turquoise) for C_4 phenanthrene and C_4 four-ring ortho-fused PASH. The same ions are minor ions of the C_2 four-ring peri-condensed PASH, see peaks marked ×. The bottom figure depicts sulfur-containing organics responding to the PFPD. Three points are addressable: (1) PAH and PASH elute within the same retention window. Ion signals from the C_4 phenanthrene, C_4 four-ring ortho-fused PASH, and C_2 four-ring peri-condensed PASH interfere with one another. Solely relying on the molecular ion or a single ion ratio produces incorrect concentrations. (2) Even with the aid of a sulfur-specific detector such reliance will still lead to false positives and negatives. (3) To obtain correct concentrations, more than one fragmentation pattern per homologue is required to assign peaks and eliminate matrix contributions to peak area. For example, the peak area is 250 times the signal obtained by multiple patterns when one or two ions are used to identify C_4 phenanthrene in coal tar. In this example, PASH interfere with PAH quantification.

On the basis of the selectivity and accuracy problems outlined above, our objective was to build a library of retention index ranges and mass spectra that will enable scientists to correctly quantify the C_1−C_4 two-, three-, and four-ring PASH. Toward this end, we analyzed four coal tars from different manufactured gas plants and four crude oils from different regions of the world by automated sequential GC−GC/MS−PFPD. Previous work on the retention behavior of PASH provided the means to select the stationary phases and column order.[31] π−π interactions dictated separation on the 50%-phenyl/50%-methylpolysiloxane phase (C1), whereas boiling point differences caused separation on the 5%-phenyl/95%-methylpolysiloxane phase (C2), see Figure 1.

Figure 5a total ion current (TIC) chromatograms are typical of coal tar (top) and crude oil (bottom) obtained after fractionation. The three heart-cuts in Figure 5b illustrate aromatics are the primary constituents. In contrast, Figure 6 shows the crude oil before fractionation. Figures 5 and 6 demonstrate the separation procedure removed nearly all of the aliphatic and polar compounds. Fractionating the samples increased mass on column (sensitivity) and minimized matrix impact on obtaining clean spectral patterns. The remaining unresolved oil mixture contains hydrocarbons that have both aromatic and aliphatic substructures.[45−47] Since coal tar produced little unresolved mixture, it served as the primary matrix to build the library, with crude oil confirming or adding to findings.

Figure 7 describes the library building process. For coinciding MS and PFPD peaks, we determined if the spectrum was the same across the peak. If sample spectra matched known PASH spectra, retention times and fragmentation patterns were cataloged. If the sample spectrum had no match but did correspond to C_1−C_4 fragmentation pathways rationalized from the analysis of 119 PASH,[31] the pattern was recorded. When peak spectra were different from one another, the deconvolution software minimized matrix interferences due to coeluting compounds. For each homologue, we combinatorially selected three confirming ions plus the molecular ion from the ions

dx.doi.org/10.1021/ac202845x | Anal. Chem. XXXX, XXX, XXX−XXX

whose RA was >10%. The deconvolved spectrum was recorded when the following criteria for compound acceptance were met.

The relative error measures the scan-to-scan variance of target ions. It compares the relative abundance of the ions to one another at each peak scan. The RE algorithm also compares the similarity of each spectrum across the peak to establish constancy and to determine if the matrix adds signal to target ions. The closer the calculated value is to zero, the smaller the difference. The *Q*-ratio measures the difference between expected and actual areas of each confirming ion divided by the base ion area across the peak. The *Q*-value assesses the average difference between the expected and actual *Q*-ratios. The deconvolution software confirmed PASH identity when RE, *Q*-ratio, and *Q*-value were ≤ 7, $\leq 20\%$, ≥ 90, respectively. Additional description of the deconvolution software is available elsewhere.[44,48,49]

Table 1 lists the fragmentation patterns found in this study as well as those in NIST, Wiley, and the literature.[50−57] Also included are the five most likely ions to produce >10% RA for C_4 four-ring peri-condensed and ortho-fused PASH as rationalized from their fragmentation pathways. We found no instances in which these ions comaximized with the sulfur-specific detector in the eight samples analyzed. On the basis of these fragmentation patterns, Table 2 lists the PASH retention index windows using the Lee (PAH)[43] and Andersson (PASH)[42] systems. The former corresponds to MS detection, the latter to PFPD.

GC/MS analysis of the eight samples revealed dramatic differences in homologue concentration when analyzing the same data file by SIE versus MFPPH. For example, in the weathered coal tar and crude oil samples shown in Table 3, all but one false positive is independent of retention window. This result alone proves only multiple fragmentation pattern analysis correctly quantifies PASH. Without the aid of the retention windows determined as a result of this study, percent overestimation of homologue concentrations ranges from tens to thousands. Even with retention windows, overestimation will range from a few percent to hundreds of percent. The magnitude of the differences, i.e., measurement accuracy, will also vary dramatically from analyst-to-analyst, sample-to-sample, and homologue-to-homologue. In contrast, spectral deconvolution of homologue patterns with, without retention windows produces the same data regardless of the variables just mentioned.

CONCLUSIONS

Current SIM/SIE data collection and analysis methods produce inaccurate PASH concentrations. In contrast, reliance on the retention windows and mass spectrometry fragmentation patterns shown in Tables 1 and 2 enables scientists to obtain accurate estimates of alkylated PASH concentrations, which should, in turn, provide more accurate estimates of the $\sum PAH_{34}$ toxicity hazard index. Ongoing research will assess how these results impact current environmental forensics used to differentiate source materials, weathering, and liability apportionments.

AUTHOR INFORMATION

Corresponding Author

*Phone: 617-627-3474. E-mail: albert.robbat@tufts.edu.

Notes

The authors declare no competing financial interest.

ACKNOWLEDGMENTS

EPRI funded this work under contract EP-P39203/C17417, PAH Weathering. We thank Gerstel GmbH and Inc., Agilent Technologies, Shimadzu, OI Analytical, and Ion Signature Technology for making the instrumentation and software available for this research.

REFERENCES

(1) Patri, M. *Ann. Neurosci.* **2009**, *16*, 22−30.
(2) Moorthy, B. *Issues Toxicol.* **2008**, *3*, 97−135.
(3) Mahadevan, B.; Courter, L. A.; Baird, W. M. In *New Developments in Mutation Research*; Valon, C. L., Ed.; Nova Science Publishers, Inc.: Hauppauge, NY, 2007; pp 19−40.
(4) Irigaray, P.; Belpomme, D. *Carcinogenesis* **2010**, *31*, 135−148.
(5) Jacob, J. *Polycyclic Aromat. Compd.* **2008**, *28*, 242−272.
(6) Puga, A.; Ma, C.; Marlowe, J. L. *Biochem. Pharmacol.* **2009**, *77*, 713−722.
(7) Belitsky, G.; Yakubovskaya, M. *Biochemistry (Moscow)* **2008**, *73*, 543−554.
(8) Brody, J. G.; Moysich, K. B.; Humblet, O.; Attfield, K. R.; Beehler, G. P.; Rudel, R. A. *Cancer* **2007**, *109*, 2667−2711.
(9) *The Carcinogenic Effects of Polycyclic Aromatic Hydrocarbons*; Luch, A., Ed.; Imperial College Press: London, 2005.
(10) Douglas, G. S.; Burns, W. A.; Bence, A. E.; Page, D. S.; Boehm, P. *Environ. Sci. Technol.* **2004**, *38*, 3958−3964.
(11) Stout, S. A.; Graan, T. P. *Environ. Sci. Technol.* **2010**, *44*, 2932−2939.
(12) Sauer, T. C.; Michel, J.; Hayes, M. O.; Aurand, D. V. *Environ. Int.* **1998**, *24*, 43−60.
(13) Stout, S. A.; Liu, B.; Millner, G. C.; Hamlin, D.; Healey, E. *Environ. Sci. Technol.* **2007**, *41*, 7242−7251.
(14) Stout, S. A.; Wang, Z. In *Oil Spill Environmental Forensics*; Stout, S. A., Wang, Z., Eds.; Academic Press: Burlington, MA, 2007; pp 1−53.
(15) Douglas, G. S.; Stout, S. A.; Uhler, A. D.; McCarthy, K. J.; Emsbo-Mattingly, S. D.; Wang, Z. In *Oil Spill Environmental Forensics: Fingerprinting and Source Identification*; Wang, Z., Stout, S. A., Eds.; Elsevier Publishing Co.: Boston, MA, 2007; pp 257−292.
(16) Kennicutt, M. C. II. *Oil Chem. Pollut.* **1988**, *4*, 89−112.
(17) Wang, Z.; Fingas, M.; Li, K. *J. Chromatogr. Sci.* **1994**, *32*, 361−366.
(18) Wang, Z.; Fingas, M.; Page, D. S. *J. Chromatogr., A* **1999**, *843*, 369−411.
(19) Bence, A. E.; Kvenvolden, K. A.; Kennicutt, M. C. *Org. Geochem.* **1996**, *24*, 7−42.
(20) Page, D. S.; Boehm, P. D.; Douglas, G. S.; Bence, A. E.; Burns, W. A.; Mankiewicz, P. J. *Environ. Toxicol. Chem.* **1996**, *15*, 1266−1281.
(21) Boehm, P. D.; Douglas, G. S.; Burns, W. A.; Mankiewicz, P. J.; Page, D. S.; Bence, A. E. *Mar. Pollut. Bull.* **1997**, *34*, 599−613.
(22) Wang, Z.; Fingas, M.; Sigouin, L. *J. Chromatogr., A* **2001**, *909*, 155−169.
(23) Wang, Z.; Fingas, M.; Sergy, G. *Environ. Sci. Technol.* **2002**, *28*, 1733−1746.
(24) Wang, Z. D.; Fingas, M.; Lambert, P.; Zeng, G.; Yang, C.; Hollebone, B. *J. Chromatogr., A* **2004**, *1038*, 201−214.
(25) *Procedures for the derivation of ESBs for the protection of benthic organisms: PAH mixtures*; EPA/600/R-02/013; U.S. Environmental Protection Agency, Office of Research and Development: Washington, DC, 2003.
(26) *Methods for the derivation of site-specific equilibrium partitioning sediment guidelines (ESGs) for the protection of benthic organisms: Non-ionic organics*; EPA/822/R/02/042; U.S. Environmental Protection Agency, Office of Science and Technology: Washington, DC, 2004.
(27) Hawthorne, S. B.; Miller, D. J.; Kreitinger, J. P. *Environ. Toxicol. Chem.* **2006**, *25*, 287−296.
(28) Di Toro, D. M.; McGrath, J. A. *Environ. Toxicol. Chem.* **2000**, *19*, 1971−1982.

(29) Di Toro, D. M.; McGrath, J. A.; Hansen, D. J. *Environ. Toxicol. Chem.* **2000**, *19*, 1951−1970.
(30) Zeigler, C.; MacNamara, K.; Wang, Z.; Robbat, A. Jr. *J. Chromatogr., A* **2008**, *1205*, 109−116.
(31) Zeigler, C. D.; Schantz, M. M.; Wise, S.; Robbat, A. J. *Polycyclic Aromat. Compd.* **2011**, in press.
(32) Ogata, M.; Miyake, Y. *Water Res.* **1979**, *13*, 1179−1185.
(33) Ogata, M.; Miyake, Y. *Acta Med. Okayama* **1978**, *32*, 419−425.
(34) Eastmond, D. A.; Booth, G. M.; Lee, M. L. *Arch. Environ. Contam. Toxicol.* **1984**, *13*, 105−111.
(35) Sinsheimer, J. E.; Hooberman, B. H.; Das, S. K.; Savla, P. M.; Ashe, A. J. *Environ. Mol. Mutagen.* **1992**, *19*, 259−264.
(36) Swartz, C. D.; King, L. C.; Nesnow, S.; Umbach, D. M.; Kumar, S.; DeMarini, D. M. *Mutat. Res.* **2009**, *661*, 47−56.
(37) Pelroy, R. A.; Stewart, D. L.; Tominaga, Y.; Iwao, M.; Castle, R. N.; Lee, M. L. *Mutat. Res.* **1983**, *117*, 31−40.
(38) Croisy, A.; Mispelter, J.; Lhoste, J. M.; Zajdela, F.; Jacquignon, P. *J. Heterocycl. Chem.* **1984**, *21*, 353−359.
(39) Warshawsky, D. *J. Environ. Sci. Health, Part C* **1992**, *10*, 1−71.
(40) Kropp, K. G.; Fedorak, P. M. *Can. J. Microbiol.* **1998**, *44*, 605−622.
(41) Andersson, J.; Hegazi, A.; Roberz, B. *Anal. Bioanal. Chem.* **2006**, *386*, 891−905.
(42) Andersson, J. T. *J. Chromatogr., A* **1986**, *354*, 83−98.
(43) Lee, M. L.; Vassilaros, D. L.; White, C. M. *Anal. Chem.* **1979**, *51*, 768−773.
(44) Robbat, A. Jr.; Kowalsick, A.; Howell, J. *J. Chromatogr., A* **2011**, *1218*, 5531−5541.
(45) Killops, S. D.; Aljuboori, M. A. H. A. *Org. Geochem.* **1990**, *15*, 147−160.
(46) Frysinger, G. S.; Gaines, R. B.; Xu, L.; Reddy, C. M. *Environ. Sci. Technol.* **2003**, *37*, 1653−1662.
(47) Ventura, G. T.; Kenig, F.; Reddy, C. M.; Frysinger, G. S.; Nelson, R. K.; Mooy, B. V.; Gaines, R. B. *Org. Geochem.* **2008**, *39*, 846−867.
(48) Gankin, Y. V.; Gorshteyn, A.; Smarason, S.; Robbat, A. Jr. *Anal. Chem.* **1998**, *70*, 1655−1663.
(49) Robbat, A. Jr.; Smarason, S.; Gankin, Y. V. *Field Anal. Chem. Technol.* **1999**, *3*, 55−66.
(50) Schade, T.; Andersson, J. T. *J. Chromatogr., A* **2006**, *1117*, 206−213.
(51) Reinecke, M. G.; Newsom, J. G.; Almqvist, K. A. *Tetrahedron* **1981**, *37*, 4151−4157.
(52) Reinecke, M. G.; Newsom, J. G.; Chen, L.-J. *J. Am. Chem. Soc.* **1981**, *103*, 2760−2769.
(53) Tedjamulia, M. L.; Tominaga, Y.; Castle, R. N.; Lee, M. L. *J. Heterocycl. Chem.* **1983**, *20*, 1485−1495.
(54) Sinninghe Damsté, J. S.; Kock-Van Dalen, A. C.; De Leeuw, J. W.; Schenck, P. A. *J. Chromatogr., A* **1988**, *435*, 435−452.
(55) Ali, M. F.; Perzanowski, H.; Koreish, S. A. *Fuel Sci. Technol. Int.* **1991**, *9*, 397−424.
(56) Kukula, P.; Gramlich, V.; Prins, R. *Helv. Chim. Acta* **2006**, *89*, 1623−1640.
(57) Bryan, C. S.; Braunger, J. A.; Lautens, M. *Angew. Chem., Int. Ed.* **2009**, *48*, 7064−7068.

dx.doi.org/10.1021/ac202845x | *Anal. Chem.* XXXX, XXX, XXX−XXX